Watari *Earth, Planets and Space* (2022) 74:115
https://doi.org/10.1186/s40623-022-01676-5

Earth, Planets and Space

FULL PAPER

Extremely large flares/multiple large flares expected from sunspot groups with large area

Shinichi Watari*

Abstract

The possible occurrence of major space weather events, such as large solar flares within one hundred years, is studied anticipating their effects on our social facilities. However, the continuous soft X-ray (SXR) observation of flares by Geostationary Operational Environmental Satellites (GOES) started in 1975, and the period of data collection is less than 50 years. On the other hand, ground-based sunspot observations have a long history. Their duration of data collection exceeds 100 years. The possibility of the occurrence of extremely large flares is estimated using the daily sunspot area data of individual sunspot groups between 1879 and 2016 using the catalogue complied by the Debrecen Heliophysical Observatory in Hungary and the catalogue updated by Mandal, Krivova, Solanki, Shinha, and Banerjee in 2020. It had become clear that large sunspot groups with the potential to produce Carrington-class flares (areas of more than 3000 MSH) have appeared on a total of 119—139 days between 1879 and 2016, and a sunspot group with the potential to produce an X100-class flare appeared between March and April 1947. According to the past major space weather events, the large sunspot groups caused a series of multiple large flares instead of just one large flare. We tried to estimate the probabilities of occurrence of a SXR flare $\geq$ X100 for 30-, 50-, and 100-year periods to be 0.70—0.76, 0.87—0.91, and 0.98—0.99, respectively, using the complementary cumulative distribution function (CCDF) of sunspot areas for the 138-year data.

Keywords: Sunspot area, Soft X-ray solar flare, Carrington-class flare, GOES, Statistical analysis, Complementary cumulative distribution function

*Correspondence: watari@nict.go.jp

National Institute of Information and Communications Technology, 4-2-1 Nukui-Kitamachi, Koganei, Tokyo 184-8795, Japan

Graphical Abstract

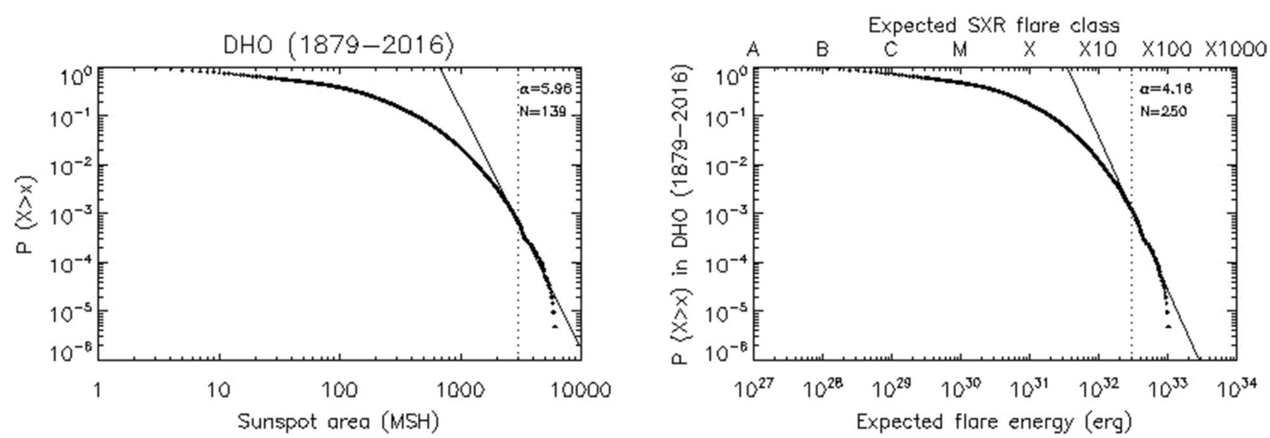

Introduction

Interest in extreme space weather events is increasing in order to mitigate their effects on our social facilities. As a result, there are many studies on extreme space weather events and their effects (Committee on the social and economic impact of severe space weather events, 2008; Hapgood 2010; Cannon et al. 2013; Knipp et al. 2021; Owens et al. 2021).

There are several approaches to studying the extreme events. One approach is to investigate the past major events in historical records. For example, the Carrington flare of 1859 (Carrington 1859) has been extensively studied as one of the largest space weather events in history, using past records (Chapman and Bartels 1940; Tsurutani et al. 2003; Boteler, 2006; Curto et al. 2016; Cliver and Svalgaard 2004; Cliver and Dietrich 2013; Hayakawa et al. 2019). Another approach is to use statistical methods for rare events. There have been several attempts to estimate the occurrence probabilities of future rare events using long-time data under the assumption of stationarity of occurrence for the time of data collection and the time in future, although Lakhina and Tsurutani (2016) noted at various publications predicting the occurrence of Carrington-like magnetic storms had significantly different results from each other. Willis et al. (1997) applied extreme value statistics for daily aa indices between 1844 and 1993. Tsubouchi and Omura (2007) applied the extreme value theory to hourly disturbance storm time (Dst) indices (Sugiura 1964) between 1957 and 2001. Love et al. (2015) fitted the Dst data (1957−2012) to the log-normal distribution.

Watari et al. (2001) calculated the return periods of large SXR flares, solar energetic particle events and magnetic storms using the Weibull distribution. Riley (2012) estimated the occurrence probabilities of extreme events such as hard X-ray solar flares, high-speed coronal mass ejections (CMEs), geomagnetic storms, and solar energetic particles (>30 MeV) using the power-law distribution of the events. Curto et al. (2016) suggested that the return period of Carrington-class flares is 90 ± 60 years on the basis of the Generalized Extreme Value (GEV) distribution applied to the flare lists between 1975 and 2015 obtained by the Geostationary Operational Environmental Satellites (GOES) of National Oceanic and Atmospheric Administration (NOAA). Kataoka (2013 and 2020) estimated the occurrence probabilities of extreme space weather events by applying the power-law and log-normal distributions to the events.

For the solar flares, the peak flux of solar X-ray (SXR) is usually used to describe their size. However, continuous SXR observation of flares by the GOES started in 1975. As a result, approximately 50 years of data are available for long-term analysis; however, we want to know events for the period of more than one hundred years. On the other hand, ground-based sunspot observations have a long history of more than one hundred years. Magnetic structure of sunspot groups is also important for occurrence of large flares. However, continuous magnetic field observations of photosphere began in the 1970s. Hence, we estimated the possibility of intense SXR flares using the long-term sunspot area data. The past records suggested that large sunspot groups tend to produce a series of multiple large flares.

Data

We used the data of daily positions and areas of individual sunspot groups over the past 143 years (1874−2016) complied by the Debrecen Heliophysical Observatory (DHO) in Hungary. Hereafter, we called it the DHO catalogue. The DHO took over the task of compiling the sunspot catalogue from the Greenwich Royal Observatory in 1976 (http://fenyi.solarobs.csfk.mta.hu/DPD/). The data between 1874 and 1976 were revised data of the Greenwich Photoheliographic Results (GPR) sunspot catalogue (Baranyi et al. 2016). The data between 1977 and 2016 were based on the Debrecen Photoheliographic Data (DPD) sunspot catalogue (Baranyi et al. 2016; Gyori et al. 2017). The data for 1977−1978, 1985−1988, 1993−2002, and 200−2015 are final ones and the data for 1979−1984, 1989−1992, 200−2004, and 2016 are preliminary ones. Mandal et al. (2020) updated the sunspot catalogue (1874−2021) using several sunspot catalogues including the GPR and DPD ones (hereafter, the MA20 catalogue; http://ww2.mps.mpg.de/project/sun-climate/data.html) and noted the data gaps in the catalogues. Hence, the MA20 catalogue was added to our analysis for comparison with the DHO catalogue. Figure 1a, b shows days of no data in the DHO and MA20 catalogues. There are similar data gaps between 1874 and 1976 because both catalogues are based on the GPR catalogue. There are large data gaps of more than 30 days in 1874−1876 and 1878 (declining phase of solar cycle 11) and there are almost isolated 1- or 2-day data gaps after 1879. We decided to exclude the data period between 1874 and 1878 from our analysis.

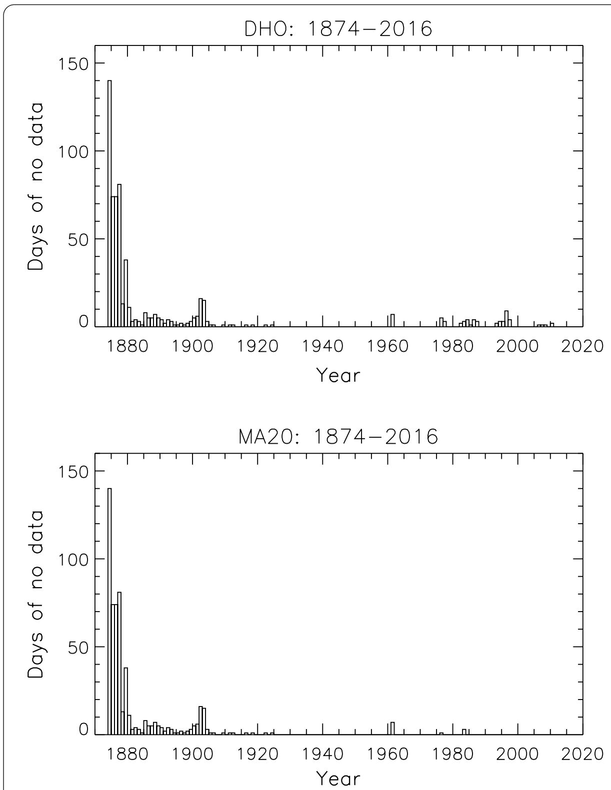

Fig. 1 Days of no data in the DHO (upper panel) and MA20 (lower panel) catalogues

We selected the sunspot groups within the longitude of 60 degrees to avoid uncertainty near the solar limbs in our analysis. Figure 2a shows yearly sunspot number, yearly number of sunspot areas of more than 1000 millionths of solar hemisphere (MSH), and yearly maximum area of sunspot groups in the DHO catalogue. Figure 2b shows the same data in the MA20 catalogue. Yearly sunspot number was obtained from the WDC-SILSO, Royal Observatory of Belgium, Brussels (https://wwwbis.sidc.be/silso/home). According to Figs. 2a, b, the sunspot group with the largest area of 6,132 MSH occurred in 1947 (maximum of solar cycle 18), whereas the largest yearly sunspot number of 269.3 was in 1957 and the largest number of sunspot areas of more than 1000 MSH of 181 occurred in 1959 around maximum of solar cycle 19. We noted that five geomagnetic storms with minimum Dst of less than −400 nT were observed in 1957, 1958, 1959, 1989, and 2003, respectively, and three of them occurred around maximum of solar cycle 19.

Sunspot area and soft X-ray peak intensity of flares

It is known that large flares tend to occur in sunspot groups with large area. Sammis et al. (2000) showed that there is an empirical relationship between the area of sunspot groups and the SXR peak intensity of solar flares from those groups. Shibata et al. (2013) noted that the upper limit of the SXR peak intensity of a flare observed by GOES (SXR flare class) can be determined using the scaling law shown by Eq. (1) if we assume that the intensity is in proportion to the total energy released by a flare (e.g., C-class: 10^{29} erg, M-class: 10^{30} erg, X-class: 10^{31} erg, X10-class: 10^{32} erg, X100-class: 10^{33} erg, and X1,000-class: 10^{34} erg):

$$E_{flare} \approx fE_{mag} \approx f\frac{B^2}{8\pi}A_{spot}^{\frac{3}{2}}. \quad (1)$$

Here, f is the fraction of magnetic energy (E_{mag}) that can be released as flare energy (E_{flare}), B is the magnetic field strength, and A_{spot} is the area of the sunspot group.

Maehara et al. (2012) found superflares (flares with energy of more than 10^{33} erg) on solar-type stars using NASA's Kepler mission data and Notsu et al. (2013) showed that the energy in the superflares is related to the total coverage of the Starspot and the superflares follow the same scaling law as shown by Eq. (1).

Tables 1, 2 summarize the sunspot groups with maximum area of more than 3000 MSH between 1879 and 2016 recorded in the DHO and MA20 catalogues and the expected maximum SXR flares calculated using Eq. (1) with B of 1000 G and f of 0.1, considering Fig. 2 in Shibata et al. (2013). Maximum SXR flares and number of X-class flares from the sunspot groups are also shown in Tables 1, 2 using the GOES flare reports available from the National Centers for Environmental Information (NCEI), NOAA (https://ngdc.noaa.gov/ngdc.html). They showed that the large sunspot groups produced a number of large flares. The sunspot group (no. 7 in Table 1/no. 4 Table 2) and associated with the 13 March 1989 magnetic storm had its maximum area of 4201/4823 MSH on

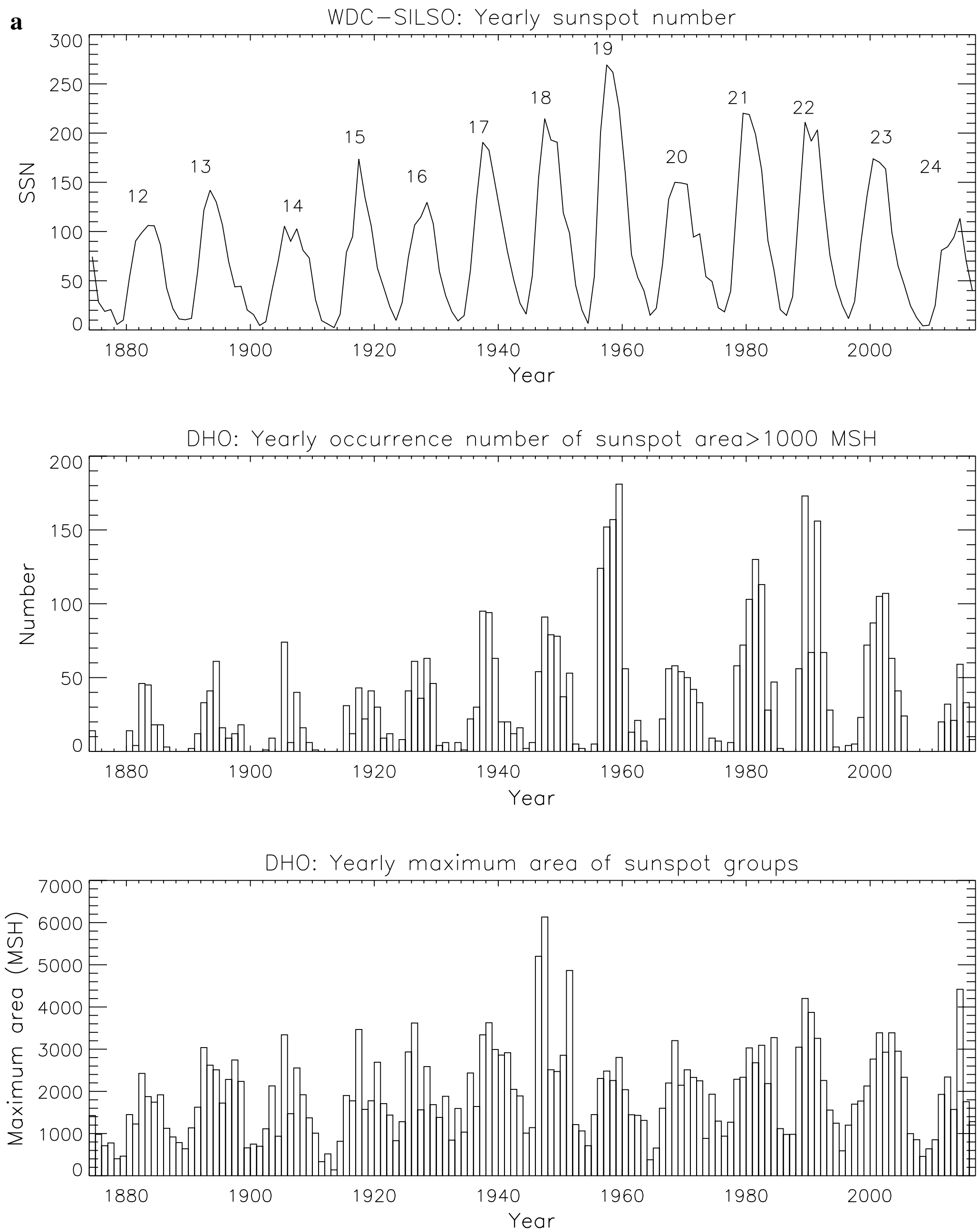

Fig. 2 **a** Yearly sunspot number, yearly number of sunspot areas of more than 1000 MSH, and yearly maximum area of sunspot groups in the DHO catalogue. **b** Yearly sunspot number, yearly number of sunspot area of more than 1000 MSH, and yearly maximum area of sunspot groups in the MA20 catalogue

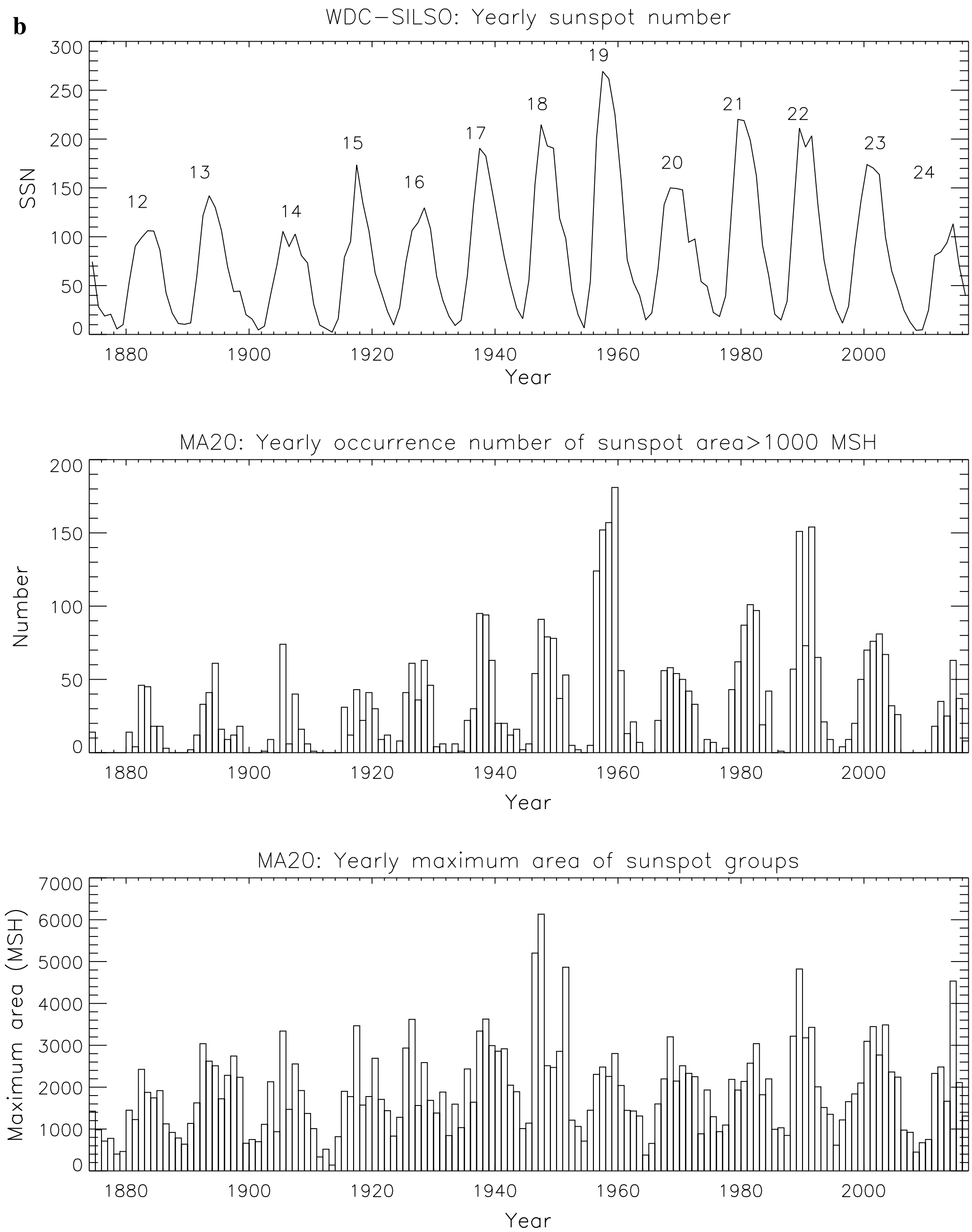

Fig. 2 continued

14 March 1989/16 March 1989. This sunspot group produced multiple large SXR flares including the maximum flare of X15 on 6 March 1989. The magnetic storm of the minimum Dst of −589 nT caused by interplanetary CMEs in association with these large flares is the largest storm since the Dst index was initiated (Lakhina and Tsurutani 2016). A power blackout occurred in Quebec, Canada, during this storm (Boteler 2019).

The sunspot group (no. 12 in Table 1/no. 11 in Table 2, NOAA active region no.10486) had its maximum area of 3388/3486 MSH on 1 November 2003/29 October 2003 and produced large flares during the Halloween event from the end of October to the beginning of November 2003. This group produced a series of large flares: an X17 flare on 28 October, X10 flare on 29 October, X8.3 flare on 2 November, and X28 flare on 4 November according

Table 1 Sunspot groups with maximum area of more than 3000 MSH and expected and observed maximum SXR flare class between 1879 and 2016 in the DHO catalog

No.	Date	Maximum sunspot area (MSH)	Expected maximum SXR flare class	Region number	Observed maximum SXR flare (number of X-class flares)
1	1947/04/08	6132	X106.3	14,886	NA
2	1946/02/07	5202	X83.1	14,417	NA
3	1951/05/19	4865	X75.1	16,763	NA
4	1946/07/29	4720	X71.8	14,585	NA
5	1947/03/12	4554	X68.0	14,851	NA
6	2014/10/24	4419	X65.0	12,192	X2.0 (4)
7	1989/03/14	4201	X60.3	5395	X15 (11)
8	1990/11/16	3872	X53.3	6368	M7.5 (0)
9	1938/01/21	3627	X48.4	12,673	NA
10	1926/01/20	3619	X48.2	9861	NA
11	1917/02/13	3467	X45.2	7977	NA
12	2003/11/01	3388	X43.7	10,486	X28 (7)
13	2001/03/29	3387	X43.6	9393	X20 (3)
14	1937/10/05	3340	X42.7	12,553	NA
15	1905/02/02	3339	X42.7	5441	NA
16	1937/07/28	3303	X42.0	12,455	NA
17	1984/04/26	3274	X41.5	4474	X13 (3)
18	1991/03/23	3257	X41.1	6555	X9.4 (7)
19	1989/06/16	3249	X41.0	5528	M9.3 (0)
20	1991/10/27	3234	X40.7	6891	X6.1 (5)
21	1968/02/01	3202	X40.1	21,482	NA
22	1917/08/09	3178	X39.7	8181	NA
23	1982/07/11	3092	X38.1	3804	X9.8 (5)
24	1988/07/02	3047	X37.2	5060	M9.2 (0)
25	1892/02/10	3038	X37.1	2421	NA
26	1980/11/13	3030	X36.9	2779	X9.0 (4)
27	1938/10/12	3003	X36.4	13,024	NA

NA: not available

to the report of NOAA. The 28 October flare produced the largest increase in total electron content (TEC) of the ionosphere in those flares (Tsurutani et al. 2005), and the storm associated with the 29 October flare produced a drastic TEC increase (Mannucci et al. 2005). During the 4th November flare, the GOES X-ray detectors were saturated. As a result, the SXR class was determined to be X28 by extrapolation. However, Thomson et al. (2004) estimated the SXR class of this flare to be X45 using the ionospheric D-region reflection height determined from the phase shifts of the very low frequency (VLF) radio signal. The minimum Dst of the associated storm was −69 nT because the flare location was S19W83 and the main portion of the CME was directed south-west.

As shown in Tables 1, 2 the sunspot group with the largest area of 6132 MSH was observed on 8 April 1947 and the expected maximum flare class was X106. Between 1879 and 2016, a sunspot area having a potential of more than X100 (of more than 5587 MSH) was observed only in this sunspot group for four days; 5785 MSH on 3 April, 5764 MSH on 5 April, 5931 MSH on 7 April, and 6132 MSH on 8 April. This suggests that the sunspot group with a potential for producing a SXR flare exceeding X100 appeared in the past, on the basis of the sunspot observation data. Unfortunately, there was no SXR observation before 1975, except ground-based H-ALPHA flare observations. Many flares of the optical importance of 1 and 2 were reported in the H-ALPHA flare reports archived by the NCEI, NOAA. However, no flare of the optical importance of 3 or 4 was reported from this group. Aulanier et al. (2013) noted that it was difficult for this group to energize as a whole because of the complex distribution of small filaments. They also noted that the upper limit of solar flare energy was ~ 6×10^{33} erg (~ X600 class), as determined from a numerical magnetohydrodynamic simulation assuming

Table 2 Sunspot groups with maximum area of more than 3000 MSH and expected and observed maximum SXR flare class between 1879 and 2016 in the MA20 catalogue

No.	Date	Maximum sunspot area (MSH)	Expected maximum SXR flare class	Region number	Observed maximum SXR flare (number of X-class flares)
1	1947/04/08	6132	X106.3	14,886	NA
2	1946/02/07	5202	X83.1	14,417	NA
3	1951/05/19	4865	X75.1	16,763	NA
4	1989/03/16	4823	X74.1	5395	X15 (11)
5	1946/07/29	4720	X71.8	14,585	NA
6	1947/03/12	4554	X68.0	14,851	NA
7	2014/10/25	4534	X67.6	12,192	X2.0 (4)
8	1989/06/16	3753	X50.9	5528	M9.3 (0)
9	1938/01/21	3627	X48.4	12,673	NA
10	1926/01/20	3619	X48.2	9861	NA
11	2003/10/29	3486	X45.6	10,486	X28 (7)
12	1917/02/13	3467	X45.2	7977	NA
13	2001/03/30	3447	X44.8	9393	X20 (3)
14	1991/10/27	3428	X44.4	6891	X6.1 (5)
15	1937/10/05	3340	X42.7	12,553	NA
16	1905/02/02	3339	X42.7	5441	NA
17	1937/07/28	3303	X42.0	12,455	NA
18	1991/03/23	3233	X40.7	6555	X9.4 (7)
19	1988/07/01	3217	X40.4	5060	M9.2 (0)
20	1968/02/01	3202	X40.1	21,482	NA
21	1990/11/20	3179	X39.7	6368	M7.5 (0)
22	1917/08/09	3178	X39.7	8181	NA
23	1989/09/04	3098	X38.2	5669	X1.3 (3)
24	2000/09/23	3096	X38.1	9169	X1.2 (1)
25	1982/06/15	3039	X37.1	3776	X3.6 (5)
26	1892/02/10	3038	X37.1	2421	NA
27	1938/10/12	3003	X36.4	13,024	NA

NA: not available

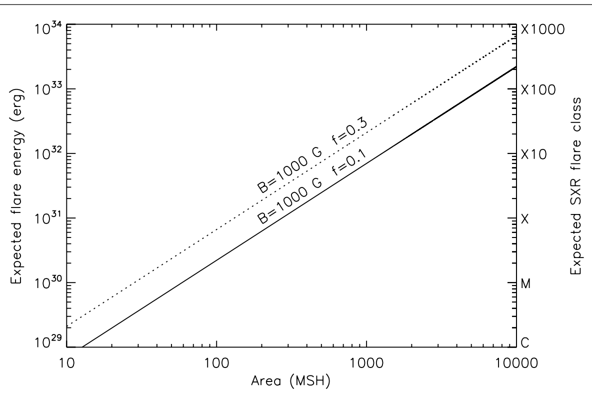

Fig. 3 Relationship between sunspot area and expected flare energy or SXR flare class calculated from the sunspot area

the largest sunspot magnetic field from the past measurements and 30% of the energy of this sunspot group to be flare energy.

Figure 3 shows the relationship between the area of sunspot groups and the expected flare energy or SXR flare class calculated using Eq. (1). The solid line is the case of $B = 1000$ G and $f = 0.1$ and the dashed line is the case of $B = 1000$ G and $f = 0.3$. Kataoka (2020) assigned the 100-year flare class as X70 from the log-normal fit to the cumulative distribution of the SXR flares using the GOES flare data between 1975 and 2016. Tables 1, 2 show that there were four/five sunspot groups with area exceeding 4600 MSH, which had the potential for producing a SXR flare of more than X70, during the past 138 years. In the DHO/MA20 catalogue, there were

21/22 days when sunspot groups with areas of more than 4600 MSH appeared on the solar disk during the past 138 years (50,179/50,225 days considering the data gaps). This means that for a period of 100 years, there are approximately 11/12 days on which sunspot groups with areas of more than 4600 MSH occur.

SXR flare class of more than X50 is expected from sunspot groups with area of more than 3700 MSH according to Eq. (1) with B of 1000 G and f of 0.1. Table 3 shows the observed number of sunspot areas of more than 3700 MSH for four selected data sets of 100-year periods. The same number of 3700 MSH sunspot areas was found in the DHO and MA20 catalogues. The number of 44 ± 2.9 seems to be large compared with the historical records of extreme magnetic storms based on ground-based geomagnetic observations (Table 1 in Tsurutani et al. (2003); Table 1 in Knipp et al. (2021)).

Several reasons are considered regarding this.

One reason is that f in Eq. (1) varies depending on the magnetic structure of the sunspot groups, as noted by Aulanier et al. (2013) on the March−April 1947 sunspot group.

The second reason is that a strong southward interplanetary magnetic field (IMF) is necessary for the occurrence of intense magnetic storms (Tsurutani et al. 2003). For example the historically fast CME associated with the flare of optical importance 3B on 4 August 1972 took approximately 14.6 h to hit Earth (Vaisberg and Zastenker, 1976; Knipp et al. 2018). However, the minimum value of Dst was only −125 nT because the IMF pointed mostly northward (Tsurutani et al. 1992).

The third reason is that the CMEs miss Earth, such as the back-side events of the sun. The 23 July 2012 event is an example of a back-side event (Russell et al. 2013; Baker et al. 2013; Ngwira et al. 2013). This event was observed by NASA's Solar Terrestrial Relations Observatory-Ahead (STEREO-A). The extremely fast CME with strong IMF reached STEREO-A (∼ 1 AU) in approximately 19 h.

Area of sunspot group associated with Carrington flare

The Carrington flare is considered to be one of the largest flares in history (Tsurutani et al. 2003; Cliver and Svalgaard 2004; Boteler 2006; Cliver and Dietrich 2013; Curto et al. 2016; Lakhina and Tsurutani 2018; Hayakawa et al. 2019). An intense magnetic storm of a minimum Dst of−1760 nT occurred 17.5 h after the white-light flare (Tsurutani et al. 2003). An examination of aurora observations associated with this flare suggests that the equatorward boundary of the aurora moved to the lowest latitude on records (Kimball 1960; Green and Boardsen 2006; Hayakawa et al. 2018, 2019).

We measured the area of the sunspot group associated with the Carrington flare using the sunspot drawing in Fig. 2 of Hayakawa et al. (2019). The measured sunspot area was approximately 3000 MSH. In the DHO/MA20 catalogue, there were 139/119 days when sunspot groups with areas of more than 3000 MSH appeared on the solar disk between 1879 and 2016.

The energy of the flare calculated using Eq. (1) assuming B of 1000 G and f of 0.1 is 3.6×10^{32} erg. This energy corresponds to the SXR peak intensity of X36. This SXR peak intensity is close to that of X45 estimated by Cliver and Svalgaard (2004), Boteler (2006), Cliver and Dietrich (2013), and Curto et al. (2016). They estimated the SXR flare size using the amplitude of rapid geomagnetic field variations associated with the SXR flares. The geomagnetic variations are produced by the enhancement of ionospheric currents induced by solar flare radiation, which is called the solar flare effect (SFE).

Statistical analysis using complementary cumulative distribution function

We applied the statistical method of Riley (2012) to the sunspot area data. For this analysis, it is necessary to use a long data period to avoid the effect of the solar cycle (∼ 11 years) variations of the sunspot area data and stationarity of occurrence is assumed for the data period and the extrapolated future period. If the probability of

Table 3 Number of sunspot area more than 3700 MSH for 100-year periods in the DHO and MA20 catalogues

Data period	Number of sunspot area of more than 3700 MSH in the DHO catalogue	Number of sunspot area of more than 3700 MSH in the MA20 catalogue
1879−1978	41	41
1889−1988	41	41
189−1998	46	46
1909−2008	46	46
Average	44 ± 2.9	44 ± 2.9

the occurrence of large-amplitude events, *p(x)*, follows a power-law distribution, the cumulative distribution function, *P(x)*, which express the probability of an event of magnitude equal to or greater than the critical value, x_{crit}, also follows a power-law distribution:

$$p(x) = Cx^{-\alpha}, \quad (2)$$

$$P(x \geq x_{crit}) = \int_x^{\infty} p\left(x'\right) dx' = \frac{C}{\alpha - 1} x^{-\alpha+1}. \quad (3)$$

Here, x is an event amplitude, α is a spectral index, and C is a constant.

The slope is calculated as,

$$\alpha - 1 = N_P \left[\sum_{i=1}^{N_P} \ln\left(\frac{x_i}{x_{min}}\right) \right]^{-1}, \quad (4)$$

where x_i is the measured value of x, N_P is the total number of events for $x \geq x_{min}$, and x_{min} is some appropriate minimum value of x below the breakdown of the power-law relationship. The expected number of events equal to or larger than a certain threshold during the data period is:

$$E(x \geq x_{crit}) = N_P P(x \geq x_{crit}). \quad (5)$$

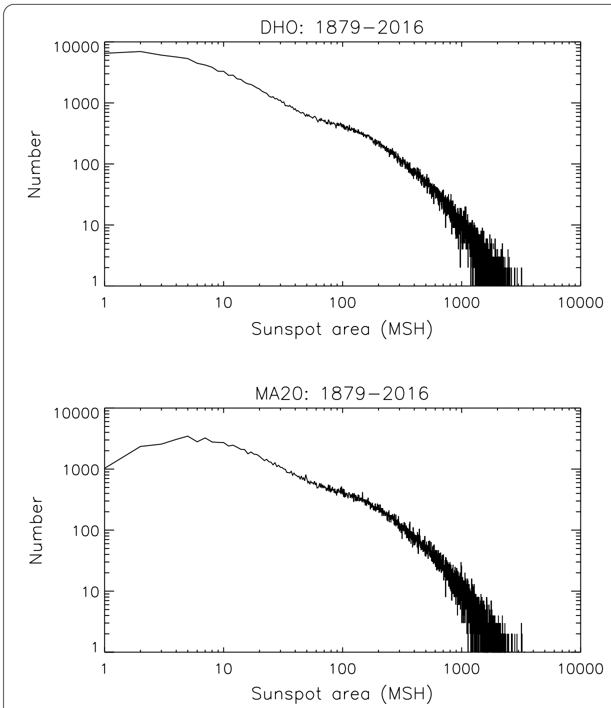

Fig. 4 Histogram of occurrence number as a function of sunspot area in the DHO (upper panel) and MA20 (lower panel) catalogues

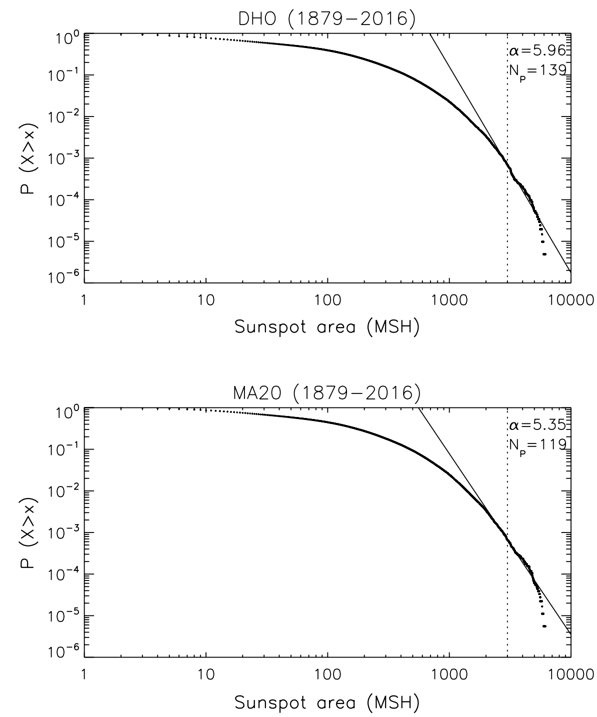

Fig. 5 Complementary cumulative distribution of occurrence number as a function of sunspot area in the DHO (upper panel) and MA20 (lower panel) catalogues. N_P is the total data number for sunspot area ≥ 3000 MSH

The probability of one or more events greater than x_{crit} occurring during a certain time period Δt is:

$$P(x \geq x_{crit}, t = \Delta t) = 1 - e^{-N_P \frac{\Delta t}{\tau} P(x \geq x_{crit})}, \quad (6)$$

where τ is the total time span of the data set and needs to be estimated by considering data gaps in the data set.

Harvey and Zwaan (1993) noted the power-law distribution of sunspot areas, whereas Bogdan et al. (1988) suggested a log-normal distribution for them. Figure 4 is histograms of the number of sunspot groups as a function of their area between 1879 and 2016 for the DHO and MA20 catalogues. Two histograms show almost the same distribution above the area of 30 MSH. Figure 5 shows the complementary cumulative distribution functions (CCDFs) of the sunspot areas shown in Fig. 4. For the CCDF in Fig. 5, α above x_{min} of 3000 MSH is calculated using Eq. (4). Table 4 shows the probabilities of the occurrence of a sunspot group with area ≥ 6000 MSH for the next 30-, 50-, and 100-year periods calculated using 80-, 100-, 120-, and 138 year data sets and Eq. (6). Table 4 shows that the estimated probabilities depend on length of the data periods.

Figure 6 shows the CCDFs of the flare energy or SXR flare size applying Eq. (1) with B of 1000 G and f of 0.1 to

Table 4 Probabilities of a sunspot group with area ≥ 6000 MSH for next 30-, 50-, and 100-year periods for 80-, 100-, 120-, and 138-year data sets in the DHO and MA20 catalogues

Data length	Occurrence probability of sunspot area ≥ 6000 MSH calculated using the DHO catalog			Occurrence probability of sunspot area ≥ 6000 MSH calculated using the MA30 catalog		
	30 years	50 years	100 years	30 years	50 years	100 years
80 years (1879–1958)	0.89	0.97	1.00	0.89	0.97	1.00
100 years (1879–1978)	0.82	0.94	1.00	0.82	0.94	1.00
120 years (1879–1998)	0.66	0.84	0.97	0.75	0.90	0.99
138 years (1879–2016)	0.62	0.80	0.96	0.72	0.88	0.99

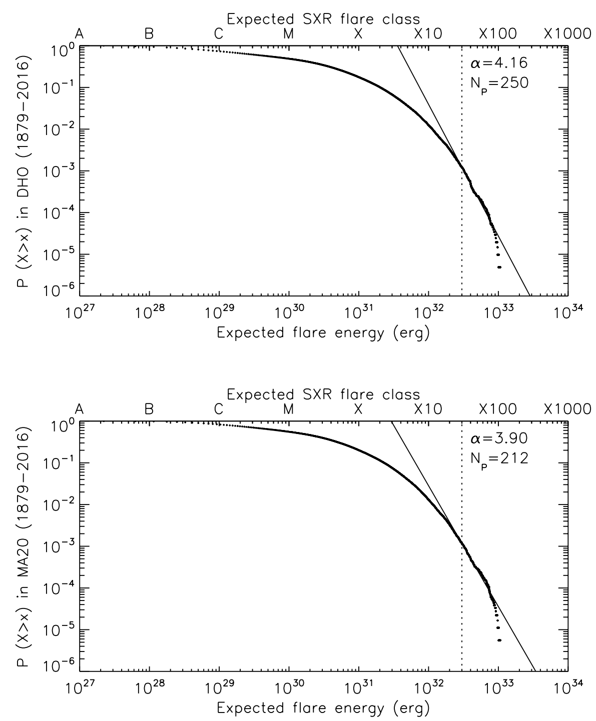

Fig. 6 Complementary cumulative distribution of occurrence number as a function of flare energy or SXR flare class calculated from sunspot area in the DHO (upper panel) and MA20 (lower panel) catalogues. N_P is the total data number for SXR flare class ≥ X30

data in Fig. 4. For the CCDF in Fig. 6 , α above x_{min} of X30 is calculated using Eq. (4). Table 5 shows the probabilities of the occurrence of a SXR flare ≥ X100 for the next 30-, 50-, and 100-year periods determined using 80-, 100-, 120-, and 138-year data sets and Eq. (6).

Summary

There are long-term ground-based observations of the area of sunspot groups compared with SXR flare observations. The possibility of the occurrence of large SXR flares was estimated using the sunspot area data collected over more than 100 years, assuming extreme flares to be related to areas of sunspot groups.

Our result suggested that sunspot groups with a potential of producing Carrington-class flares (areas of more than 3000 MSH) were observed on a total of 119−139 days between 1879 and 2016, and a sunspot group with the potential of producing an X100-class flare appeared between March and April 1947. The past records showed that the large sunspot groups produced not only one large flare, but also multiple large flares.

The SXR flare class of the Carrington flare was estimated using the sunspot area of 3000 MSH. The estimated SXR flare class of X36 is close to that of X45 estimated using the amplitude of the SFE (Cliver and

Table 5 Probabilities of a SXR flare ≥ X100 for next 30-, 50-, and 100-year periods for 80-, 100-, 120-, and 138-year data sets in the DH and MA20 catalogues

Data length	Occurrence probability of sunspot area ≥ X100 calculated using the DHO catalog			Occurrence probability of sunspot area ≥ X100 calculated using the MA30 catalog		
	30 years	50 years	100 years	30 years	50 years	100 years
80 years (1879–1958)	0.92	0.99	1.00	0.92	0.99	1.00
100 years (1879–1978)	0.85	0.96	1.00	0.85	0.96	1.00
120 years (1879–1998)	0.73	0.89	0.99	0.74	0.90	0.99
138 years (1879–2016)	0.70	0.87	0.98	0.76	0.91	0.99

Svalgaard 2004; Boteler 2006; Cliver and Dietrich 2013; Curto et al. 2016).

We also calculated the probability of the occurrence of large flares using the sunspot area data. For the 138-year dataset, the expected occurrence probabilities of a SXR flare $\geq$ X100 over the next 30-, 50-, and 100-year periods were 0.70−0.76, 0.87−0.91, and 0.91−0.99, respectively, although the estimated probabilities depend on length of the data periods.

Abbreviations

CCDF: Complementary cumulative distribution function; CME: Coronal mass ejection; DHO: Debrecen Heliophysical Observatory; DPD: Debrecen Photoheliographic Data; Dst index: Disturbance storm time index; GEV: Generalized extreme value; GOES: Geostationary Operational Environmental Satellites; GPR: Greenwich Photoheliographic Results; IMF: Interplanetary magnetic field; MSH: Millionths of solar hemisphere; NCEI: National Centers for Environmental Information; NOAA: National Oceanic and Atmospheric Administration; SFE: Solar flare effect; SSN: Sunspot number; SXR: Soft X-ray; TEC: Total electron content; VLF: Very low frequency.

Acknowledgements

We thank the Debrecen Heliophysical Observatory in Hungary for the long-term sunspot area data, WDC-SILSO, Royal Observatory of Belgium, Brussels for the yearly sunspot data, and the solar flare reports for the NCEI, NOAA. We also thank Mandel, Krivova, Solanki, Shinha, and Banerjee for their effort in updating the catalogue of the daily individual sunspot areas. We acknowledge the anonymous reviewers for helpful suggestions on this manuscript.

Author contributions

SW analyzed the data and wrote the manuscript. All author read and approved the final manuscript.

Funding

No funding.

Availability of data and materials

The long-term daily sunspot area data of individual sunspot groups are available from the Debrecen Heliophysical Observatory in Hungary (http://fenyi.solarobs.csfk.mta.hu/DPD/). The daily data of individual sunspot areas updated by Mandel et al. (2020) are from the Solar Variability and Climate Research Group, Department of Sun and Heliosphere, the Max Planck Institute for Solar System Research (http://www2.mps.mpg.de/projects/sun-climate/data.html). The yearly sunspot number data are available from the WDC-SILSO, Royal Observatory of Belgium (https://wwwbis.sidc.be/silso/home). The solar flare reports are archived by the NCEI, NOAA (https://ngdc.noaa.gov/ngdc.html).

Declarations

Ethics approval and consent to participate

Not applicable.

Consent for publications

Not applicable.

Competing interests

No competing interests.

Received: 11 January 2022 Accepted: 10 July 2022
Published online: 25 July 2022

References

Aulanier G, Demoulin P, Schrijver CJ, Janvier M, Pariat E, Schmieder B (2013) The standard flare model in three dimensions II. Upper Limit Sol Flare Energy. https://doi.org/10.1051/0004-6361/202120406

Baker DN, Li X, Pulkkinen A, Ngwira CM, Mays ML, Galvin AB, Simunac KDC (2013) A major solar eruptive event in July 2012: defining extreme space weather scenarios. Sp Weather 11(10):585–591. https://doi.org/10.1002/swe.20097

Baranyi T, Győri L, Ludmány A (2016) On-line tools for solar data compiled at the Debrecen observatory and their extensions with the Greenwich sunspot data. Solar Phys 291:3081–3102. https://doi.org/10.1007/s11207-016-0930-1

Bogdan TJ, Gilman PA, Lerche I, Howard R (1988) Distribution of sunspot umbral areas: 1917–1982. Astrophys J 327:451–456. https://doi.org/10.1086/166206

Boteler DH (2006) The super storms of august/september 1859 and their effects on telegraph system. Adv Space Res 38(2):159–172. https://doi.org/10.1016/j.asr.2006.01.013

Boteler DH (2019) A 21st century view of the march 1989 magnetic storm. Space Weather 17(10):1427–1441. https://doi.org/10.1029/2019SW002278

Cannon PS et al (2013) Extreme space weather: impacts on engineering systems. Royal Academy of Engineering, London (**1-903496-95-0**)

Carrington RC (1859) Description of a singular appearance seen in the sun on september 1, 1859. Mon Not R Astron Soc 20(1):13–15. https://doi.org/10.1093/mnras/20.1.13

Chapman S, Bartels J (1940) Geomagnetism. Oxford Univ Press, New York

Cliver EW, Dietrich F (2013) The 1859 space weather event revisited: limits of extreme activity. J Space Weather Space Clim 3:A31. https://doi.org/10.1051/swsc/2013063

Cliver EW, Svalgaard L (2004) The 1859 solar-terrestrial disturbance and the current limits of extreme space weather activity. Solar Phys 224(1–2):407–422. https://doi.org/10.1007/s11207-005-4980-z

Committee on the social and economic impacts of severe space weather events (2008) Severe space weather events -Understanding social and economic impacts: a workshop report. National Academies Press, Washington D C

Curto JJ, Castell J, Del Moral F (2016) SFE: waiting for the big one. J Space Weather Space Clim 6:A23. https://doi.org/10.1051/swsc/2016018

Green JL, Boardsen S (2006) Duration and extent of the great auroral storm of 1859. Adv Space Res 38(2):130–135. https://doi.org/10.1016/j.asr.2005.08.054

Győri L, Ludmány A, Baranyi T (2017) Comparative analysis of debrecen sunspot catalogues. Mon Not R Astron Soc 465(2):1259–1273. https://doi.org/10.1093/mnras/stw2667

Hapgood MA (2010) Space weather: its impact on earth and implications for business. Lloyd's, London

Harvey K, Zwaan C (1993) Properties and emergence patterns of bipolar active regions i size distribution and emergence frequency. Solar Phys 148(1):85–118. https://doi.org/10.1007/BF00675537

Hayakawa H, Ebihara Y, Hand DP, Hayakawa S, Kumar S, Mukherjee S, Veenadhari B (2018) Low-latitude aurorae during the extreme space weather events in 1859. Astron J 869(1):57. https://doi.org/10.3847/1538-4357/aae47c

Hayakawa H, Ebihara Y, Willis DM, Toriumi S, Iju T, Hattori K, Wild MN, Oliveira DM, Ermolli I, Ribeiro JR, Correia AP, Ribeiro AI, Knipp DJ (2019) Temporal and spatial evolutions of a large sunspot and great auroral storms around the Carrington event in 1859. Space Weather 17(11):1553–1569. https://doi.org/10.1029/2019SW002269

Kataoka R (2013) Probability of occurrence of extreme magnetic storms. Space Weather 11(5):214–218. https://doi.org/10.1002/swe.20044

Kataoka R (2020) Extreme geomagnetic activities: a statistical study. Earth Planets Space 72(5):124. https://doi.org/10.1186/s40623-020-01261-8

Kimball DS (1960) A study of the aurora of 1859 Sci Rpt 6 UAG-R109. Univ Alaska Fairbanks, Alaska

Knipp DJ, Fraser BJ, Shea MA, Smart DF (2018) On the little-known consequences of the 4 August 1972 ultra-fast coronal mass ejecta; facts, commentary, and call to action. Space Weather 16(11):1635–1643. https://doi.org/10.1029/2018SW002024
Knipp DJ, Bernstein V, Wahl K, Hayakawa H (2021) Timelines as a tool for learning about space weather storms. J Space Weather Space Clim 11:29. https://doi.org/10.1051/swsc/2021011
Lakhina GS, Tsurutani BT (2016) Geomagnetic storms: historical perspective to modern view. Geosci Lett 3:5. https://doi.org/10.1186/s40562-016-0037-4
Lakhina GS, Tsurutani B (2018) Supergeomagnetic storms: Past, present, and future. In: Buzulukova N (ed) Extreme events in geospace: origins, predictability, and consequences. Elsevier, Amsterdam, pp 157–184
Love JL, Rigler EJ, Pulkkinen A, Riley P (2015) On the lognormality of historical magnetic storm intensity statistics: Implications for extreme-event probabilities. Geophys Res Lett 42:6544–6553. https://doi.org/10.1002/2015GL064842
Maehara H, Shibayama T, Notsu S, Notsu Y, Nagao T, Kusaba S, Honda S, Nogami D, Shibata K (2012) Superflares on solar-type stars. Nature 485:478. https://doi.org/10.1038/nature11063
Mandal S, Krivova NA, Solanki SK, Sinha N, Banerjee D (2020) Sunspot area catalogue revisited: daily cross-calibrated areas since 1874. A&a 640:A78. https://doi.org/10.1051/0004-6361/202037547
Mannucci AJ, Tsurutani BT, Iijima BA, Komjathy A, Saito A, Gonzalez WD, Guarnieri FL, Kozyra JU, Skoug R (2005) Dayside global ionospheric response to the major interplanetary events of october 29–30, 2003 "halloween storms." Geophys Res Lett 32:L12S02. https://doi.org/10.1029/2004GL021467
Ngwira CM, Pulkkinen A, Mays ML, Kuznetsova MM, Galvin AB, Simunac K, Baker DN, Li X, Zheng Y, Glocer A (2013) Simulation of the 23 July 2012 extreme space weather event: what if this extremely rare CME was earth directed? Space Weather 11(12):671–679. https://doi.org/10.1002/2013SW000990
Notsu Y, Shibayama T, Maehara H, Notsu S, Nagao T, Honda S, Ishii TT, Nogami D, Shibata K (2013) Superflares on solar-type stars observed with KEPLER II photometric variability of superflare-generating stars a signature of stellar rotation and starspots. Astrophys J 771(2):127. https://doi.org/10.1088/0004-637X/771/2/127
Owens MJ, Lockwood M, Barnard LA, Scott CJ, Haines C, Macneil A (2021) Extreme space-weather events and solar cycle. Solar Phys 296:82. https://doi.org/10.1007/s11207-021-01831-3
Riley P (2012) On the probability of occurrence of extreme space weather events. Space Weather 10(2):S02012. https://doi.org/10.1029/2011SW000734
Russell CT, Mewaldt RA, Cohen CMS, Leske RA, Luhmann JG, Mason GM, von Rosenvinge TT, Gomez-Herrero R, Klassen A, Galvin AB, Simunac KDC (2013) The very unusual interplanetary coronal mass ejection of 2021 july 23: a blast wave mediated by solar energetic particles. Astrophys J 770(1):38. https://doi.org/10.1088/0004-637X/770/1/38
Sammis I, Tang F, Zirin H (2000) The dependence of large flare occurrence on the magnetic structure of sunspots. Astrophys J 540(1):583–587. https://doi.org/10.1086/309303
Shibata K, Isobe H, Hillier A, Choudhuri AR, Maehara H, Ishii TT, Shibayama T, Notsu S, Notsu Y, Nagao T, Honda S, Nogami D (2013) Can superflares occur on our sun? Publ Astron Soc Jpn 65(3):49. https://doi.org/10.1093/pasj/65.3.49
Sugiura M (1964) Hourly values of equatorial Dst for the IGY. Annu Intern Geophys Year 35:9–45
Thomson NR, Rodger CJ, Dowden RL (2004) Ionosphere gives size of greatest solar flares. Geophys Res Lett 31:L06803. https://doi.org/10.1029/2003GL019345
Tsubouchi K, Omura Y (2007) Long-term occurrence probabilities of intense geomagnetic storm events. Space Weather 5:S12003. https://doi.org/10.1029/2007SW000329
Tsurutani BT, Gonzalez WD, Tang F, Lee YT, Okada M, Park D (1992) Reply to L J Lanzerotti solar wind ram pressure corrections and an estimation of the efficiency of viscous interaction. Geophys Res Lett 19(19):1993–1994. https://doi.org/10.1029/92GL02239
Tsurutani BT, Gonzalez WD, Lakhina GS, Alex S (2003) The extreme magnetic storm of 1–2 September 1859. J Geophys Res 108(A7):1268. https://doi.org/10.1029/2002JA009504
Tsurutani BT, Judge DL, Guarmieri FL, Gangopadhyay P, Jones AR, Nuttall J, Zambon GA, Didkovsky L, Mannucci AJ, Iijima B, Meier RR, Immel TJ, Woods TN, Prasad S, Floyd L, Huba J, Solomon SC, Straus P, Viereck R (2005) The october 28, 2003 extreme EUV solar flare and resultant extreme ionospheric effects: comparison to other halloween events and bastille day event. Geophys Res Lett 32:L03S09. https://doi.org/10.1029/2004GL021475
Vaisberg OL, Zastenker GN (1976) Solar wind and magnetosheath observations at earth during august 1976. Space Sci Rev 19:687
Watari S, Kunitake M, Watanabe T (2001) The bastille day (14 July 2000) event in historical large sun-earth connection events. Sol Phys 204:423–436. https://doi.org/10.1023/A:1014273227639
Willis DM, Stevens PR, Crothers SR (1997) Statistics of the largest geomagnetic storms per solar cycles (1844–1993). Ann Geophysicae 15:719–728. https://doi.org/10.1007/s00585-997-0719-5

Publisher's Note

Springer Nature remains neutral with regard to jurisdictional claims in published maps and institutional affiliations.